BEILSTEIN JOURNAL OF ORGANIC CHEMISTRY

Possible bi-stable structures of pyrenebutanoic acid-linked protein molecules adsorbed on graphene: theoretical study

Yasuhiro Oishi, Motoharu Kitatani and Koichi Kusakabe*

Full Research Paper

Open Access

Address:
Graduate School of Science, University of Hyogo, Kamigori, Hyogo 678-1297, Japan

Email:
Koichi Kusakabe* - kusakabe@sci.u-hyogo.ac.jp

* Corresponding author

Keywords:
biosensor; DFT; PASE; protein; surface adsorption

Beilstein J. Org. Chem. **2024,** *20,* 570–577.
https://doi.org/10.3762/bjoc.20.49

Received: 09 December 2023
Accepted: 19 February 2024
Published: 11 March 2024

This article is part of the thematic issue "Carbon-rich materials: from polyaromatic molecules to fullerenes and other carbon allotropes".

Guest Editor: Y. Yamakoshi

Abstract

We theoretically analyze possible multiple conformations of protein molecules immobilized by 1-pyrenebutanoic acid succinimidyl ester (PASE) linkers on graphene. The activation barrier between two bi-stable conformations exhibited by PASE is confirmed to be based on the steric hindrance effect between a hydrogen on the pyrene group and a hydrogen on the alkyl group of this molecule. Even after the protein is supplemented, this steric hindrance effect remains if the local structure of the linker consisting of an alkyl group and a pyrene group is maintained. Therefore, it is likely that the kinetic behavior of a protein immobilized with a single PASE linker exhibits an activation barrier-type energy surface between the bi-stable conformations on graphene. We discuss the expected protein sensors when this type of energy surface appears and provide a guideline for improving the sensitivity, especially as an oscillator-type biosensor.

Introduction

Consideration of the atomic-scale motion of molecules based on nanoscience can lead to a better understanding of the behavior of target biomaterials and improve the sensitivity of specific dynamical systems, such as biosensors. In this study, we investigate the behavior of proteins immobilized with linker molecules on graphene substrates. It is known that graphene may not easily adsorb proteins [1]. On the other hand, proteins can be immobilized on graphene by using appropriate linker molecules, such as 1-pyrenebutanoic acid succinimidyl ester (PASE). Actually, pyrene and its derivatives have been demonstrated to form stable bindings to carbon materials [2,3]. The properties and characteristics of these linker molecules are keys

not only to the purpose of protein immobilization, but also to the behavior of the entire biosensor system.

In oscillator-based biosensors, further adsorption on the sensor, such as viruses using antigen/antibody reactions, may be detected via elastic-wave measurements. For this purpose, the antibody protein must first be immobilized on graphene. The antibody that specifically reacts with the target antigen is immobilized onto a graphene surface via the PASE linker. After that, the antigen is injected on sensor chips and specifically binds to the antibody. The antigen is then detected by observing the change in the vibrational frequency before and after the injection of the antigen.

The immobilization of a protein using a PASE linker on carbon nanotube [1], graphite [4], and graphene [5] has been reported. The adsorption of PASE has been considered to mainly come from the pyrene fragment, which forms π–π stacking on these graphitic carbon materials [6-8].

The sensitivity of the oscillator-based sensor depends on the structure of the linker molecule. Therefore, understanding the adsorption mechanism of the PASE linker on graphene and identifying characteristic conformations of the adsorbed molecules are of great importance. Recently, a research group including two of the present authors theoretically investigated the adsorption structure of PASE [9], revealing that PASE on graphene has a stable configuration (conformation 1) in a straight form on graphene. There is at least one metastable bent configuration (conformation 2) on the potential energy surface. Besides, the reaction barrier of the conformational change of the PASE was determined.

In this paper, we further examine a reaction pathway on the adiabatic potential energy surface that connects these conformations caused by the deformation of the PASE linker. The reaction pathway for the conformational change of the PASE itself was found to have a reaction activation barrier [9]. First, we identify that the origin of the barrier is the steric hindrance effect between two hydrogen atoms in the molecule.

A discussion on how the activation barrier between possible conformations of a protein immobilized on graphene by linkers appears is also provided. We consider the adsorption of the linker molecule forming a bond with a protein, and derive the sufficient conditions for the adiabatic potential energy surface to have an activation barrier.

The reaction pathway having an activation barrier has an advantage in the detection of adsorbed molecules using elastic wave measurements. We explore the conditions under which this advantage can be expected for proteins immobilized on graphene. As a result, we propose a strategy for improving the accuracy of the sensing process in elastic wave measurement sensors through antigen/antibody reactions.

Results and Discussion

PASE and PASE-derivatives on graphene

Among pyrene derivatives, PASE is widely used as a linker to connect carbon materials and proteins (Figure 1a) [1,4,5]. The PASE linker and a certain protein can be connected through a dehydration condensation reaction so that the succinimidyl ester group is replaced by an amido group with a protein (Figure 1b). This dehydration-condensed linker with the protein may be used to immobilize proteins onto graphene. Since the connecting linker becomes a pyrenebutanoic acid derivative (PBA), we will call them PBA-linked molecules. The adsorption of such molecules on graphene is known to happen by a mechanism similar to the adsorption of PASE on graphene [3,4].

The protein and pyrene are connected via an alkyl chain. The atomic configuration of this alkyl chain is believed not to be largely affected by the substitution of the succinimidyl group with an amino group. On the other hand, proteins alone do not readily form adsorbed structures on graphene [1]. Therefore, the pyrene moiety is bound to graphene, and at the same time, the protein is supplemented by a dehydration-condensed linker with the protein.

As introduced, on graphene, PASE is found to be straight as the most stable conformation (conformation1 in Figure 1c) [9]. On the potential energy surface, a curved conformation (conformation 2 in Figure 1d) exists. Our previous results suggested that conformation 2 is a metastable state. The relative stability of these conformations is known to vary depending on the surrounding environment, e.g., solvents and solutes [9].

Actually, the presence of solutes consisting of water and proteins improves the stability of conformation 2. This stabilization is explained partly by the formation of hydrogen bonds between water molecules and PASE. Conformation 2 increases the number of sites where hydrogen bonds can form with water molecules because the chain portion of PASE turns upward. Therefore, the stabilization energy of hydrogen-bond formation is greater in conformation 2 than in conformation 1.

To improve the stability of conformation 2, hydration effects by electrostatic interactions between PASE and the solvent are also important. A selective hydration of the polar moiety while keeping the pyrene moiety stable can relatively strengthen the stability of conformation 2. Thus, as the polarity of the solvent

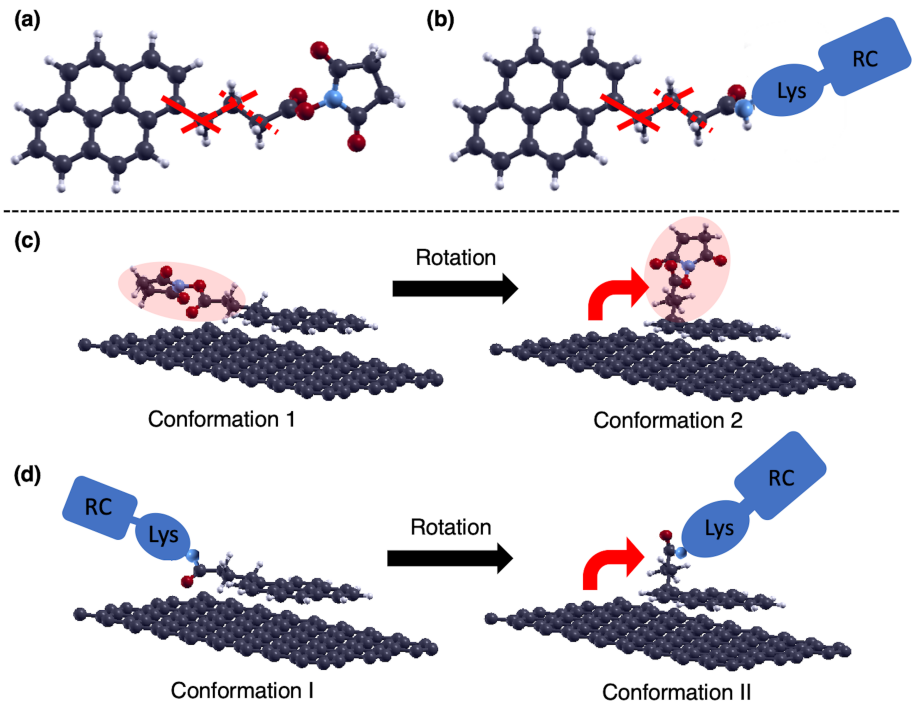

Figure 1: (a) Molecular structure of 1-pyrenebutanoic acid succinimidyl ester (PASE). The black, white, red, and blue balls represent C, H, O, and N atoms, respectively. The solid, broken, and dotted red lines represent the rotation axis. Atomic geometry is visualized by Xcrysden [10] throughout this paper. (b) Schematic diagram of the dehydration-condensation structure of a hypothetical protein and PASE. Lys indicates lysine, and RC is the active center of the antigen/antibody reaction. (c) Structures of PASE linker on graphene for conformation 1 and 2, respectively [9]. (d) Schematic PBA-linked molecular structures on graphene for conformation I and II, respectively.

increases, the probability of conformation 2 appearance is expected to increase.

Mechanism of bi-stability in PASE on graphene

Conformations of PASE are interconverted by mutual transition when the molecule is twisted around one of the carbon–carbon single bonds in the alkyl chain. The rotational motion connecting conformation 1 and conformation 2 happens around the single bond indicated by the solid red line in Figure 1a. The results of the nudged elastic band calculations show that the energy difference between the conformations is about 0.35 eV and the activation barrier on the path is about 0.55 eV (Figure 2) [9]. We will refer to the pathway on the potential energy surface with such an activation barrier as an activation barrier-type pathway.

The pathway connecting conformations 1 and 2 appears as a torsion of the alkyl chain around the carbon–carbon single bond, as indicated by the solid red line in Figure 1a. This is a kind of rotational motion. We determined the dihedral angles formed by the four carbon atoms connected by the red line in Figure 3, and the values of dihedral angles for conformations 1, 2, and the conformation at the activation barrier top are collected in Table 1. From these values, we can interpret the torsion as an approximate rotation. We call the rotations 0, $\pi/3$, and $2\pi/3$ as an approximation, where conformation 1 corresponds to a 0 rotation, conformation 2 a $2\pi/3$ rotation, and the conformation at the activation barrier top a $\pi/3$ rotation, respectively.

To confirm the origin of the activation barrier that appears between conformation 1 and 2, we discuss the structural features of the activation barrier in detail. Figure 3 shows the structure at the activation barrier top. Two hydrogen atoms connected by the green line are characteristically close to each other. One hydrogen is on the pyrene skeleton and the other is on the alkyl chain. The distance between these hydrogens is close, with about 1.8 Å (Table 1). If we compare this distance with the distance between the same hydrogen pairs in conformation 1 and conformation 2, we can see that 1.8 Å is indeed very short compared with that for the others (about 2.2 Å). Therefore, we conclude that a local steric hindrance occurs at the activation barrier.

This steric hindrance effect is analogous to the well-known steric hindrance effect of the rotation around the C–C bond in ethane. Indeed, on the graphene surface, the possible conforma-

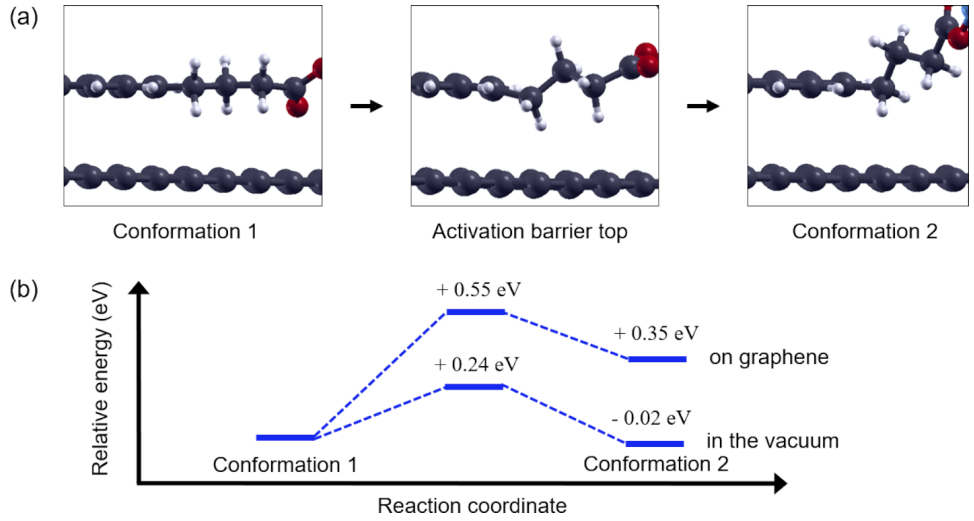

Figure 2: (a) Local structures around the butyl chain in conformation 1, the structure at activation barrier top, and conformation 2 of PASE. (b) Relative energies of PASE in a vacuum are compared to those of reported values for PASE on graphene for each conformation [9]. The energy of conformation 1 is taken as an origin.

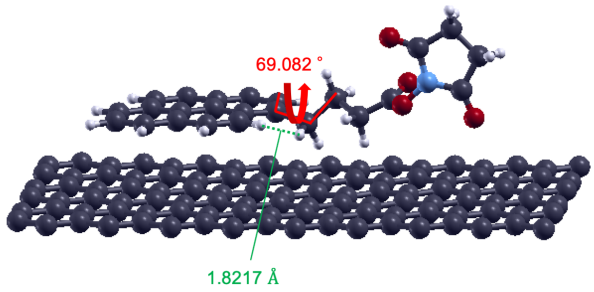

Figure 3: Structure of PASE on graphene at the activation barrier top [9]. Detailed values of the torsion angle and the distance between hydrogen atoms reveal appearance of a steric hindrance effect.

Table 1: The dihedral angles formed by the four carbon atoms connected by the red line in Figure 3, and the distance between hydrogen atoms connected by the green line in Figure 3, for conformation 1, 2, and the conformation at the activation barrier top, respectively.

Conformation	Dihedral angle [degree]	Distance between H atoms [Å]
conformation 1	3.244	2.2443
activation barrier top	69.082	1.8217
conformation 2	107.601	2.1785

tions resulting from the rotation are effectively limited to conformation 2, due, in part, to the restricted direction of rotation. In this case, the activation barrier is created by the proximity of two hydrogen atoms.

Interpretation of the steric hindrance in the molecule is certified by looking at an activation barrier caused by the rotational motion of isolated PASE. In Figure 2b, we added an estimation of the energy pathway of isolated PASE. The barrier height is around 0.2 eV. At the top of the barrier, the proximity of corresponding two hydrogen atoms happens. A reason for a higher barrier of PASE on graphene than for the isolated one is a larger exothermic adsorption energy of conformation 1 (1.63 eV), than that of conformation 2, which is about 1.28 eV. The stabilization of conformation 1 partly comes from interaction between the succinimidyl ester part and graphene.

There are other C–C single bonds in the alkyl chain, such as those shown by the dashed and dotted lines in Figure 1a. Rotations around each bond can also happen and we expect similar steric hindrance effects to appear.

Mechanical properties of PBA-linked molecular structure on graphene

Here, we discuss possible conformations of the PBA-linked molecule. Would a similar activation barrier-type potential energy surface be expected to appear in the case of succinimide substitutions by proteins? To answer this question, we consider imide substitutions extensively. In principle, if the effect of substitution only provides a weak perturbation, the potential energy surface is only slightly changed and the barrier is maintained.

A substitution effect that does not effectively change the potential energy surface is isotopic substitution. In fact, the adiabatic

potential surface defined for a hypothetical motion at the absolute zero is not changed by a change in nuclear mass. Even in density functional theory calculations, for example, the adiabatic potential energy surface, defined as the Born–Oppenheimer surface, is invariant for substitution between isotopes of carbon. This is an example of the weak perturbation.

In substitutions where the mass effect can be regarded as the predominant effect, it is safe to assume that similar steric hindrance effects appear when rotation around the alkyl chain occurs. Such an assumption may not be valid when substitutional binding of the linker to the protein causes some effects to the extent which rotation is not defined, such as a strong chemical bond change, a conformational change around the alkyl chain, or a distortion effect appearing in the adsorption structure of the linker itself. Those effects are not represented by mass substitution.

Thus, we suppose that a substitution occurs to the extent which rotational motion around a C–C single bond in the alkyl chain is defined. We assume that this is a case that can be treated as a weak perturbation that manifests itself as a mass effect. Then, two (meta-)stable conformations would appear, one with the protein-containing part linearly lying on graphene (conformation I), and the other with the conformation resulting from rotation at the alkyl chain (conformation II), as shown in Figure 1d. Rotational motion at the alkyl chain inevitably involves steric hindrance effects around the C–C bond. In particular, for motions corresponding to rotations around the C–C bond in PASE represented by the solid red line in Figure 1a and b, the magnitude of the activation barrier is expected to be close to that in PASE. This is expected to be the case since a protein weakly bound to the carbon graphitic network can be supplemented onto graphene only by linkers as PASE, which has often been observed experimentally [1]. This type of proteins is weakly coupled to graphene. It can be concluded that except for bulky structures that allow multiple binding on graphene by several linkers, the above cases will be of a weakly perturbed nature when making a single link for protein capture.

Discussion on strategy for improving biosensors

The vibrational properties of elastic waves, such as phase and amplitude, are known to be highly sensitive to the mass of adsorbed materials on multilayered graphene. Recently, a biosensor that detects target antigens by elastic wave measurement has been developed [11,12], using the method of immobilizing an antibody protein on graphitic material by a linker. The target antigen is introduced onto the sensor chips through antibody/antigen reaction. The present study is concerned with the mechanical deformation of the linker molecule. The mechanical properties of the rotational motion are almost the same whether modelled in single-layer graphene or in multilayer graphene.

Graphene has been considered as an ideal material for the platform of biosensors [13-23], benefiting from its excellent properties such as large detection area and high thermal conductivity [14,24,25]. Various biosensors have already been developed, many of which require immobilization of antibody proteins on graphene surface. Therefore, protein capture by linkers is used in a relatively large number of sensors.

In the elastic wave measurement system, elastic waves are generated by laser irradiation and their responses are observed. The elastic wave is excited by a pump light, and the response of the substrate is observed via the probe light. The refractive index of metallic substrates such as graphene may change due to the arrival of elastic waves, and this change can be observed by detecting the reflected light of the probe light. For such laser-based biosensors, graphene's conductivity can provide a unique advantage. In fact, the conductivity of multilayered graphene is highly anisotropic. Therefore, the use of multilayer graphene avoids the burning of biomaterials by lasers irradiated from the backside of the substrate.

Here, we will see how the sensitivity of this sensor can be improved when there is such rotational motion of the linked molecules adsorbed on graphene. There are two steps improved effectively by our strategy, i.e., i) creation of PBA-linked molecular structures densely on graphene, and ii) enhancement of the antigen/antibody reaction.

As already mentioned, the stability of conformation 2 of PASE is improved in solution. When the energies of two conformations come close, the activation barrier is expected to be lowered. This tendency holds in the result of Figure 2b. When a PBA-linked molecule is used, the relative energy of conformation II to that of conformation I can be better suited using our strategy.

This stabilization is explained partly by the formation of hydrogen bonds between water molecules and PASE. As in the case of PASE, the chain portion of the PBA-linked molecule turns upward, increasing the number of sites that can form hydrogen bonds with water molecules in conformation II. Therefore, the formation of hydrogen bonds can stabilize conformation II relatively more strongly than conformation I. The hydration effect also improves the stability of conformation II. Thus, as the polarity of the solvent increases, the probability of the appearance of conformation II is expected to increase. Then, conditions of the temperature and the external pressure of gases have to be chosen properly, too. We need to keep the pyrene part

stable in the whole procedures while activating the rotational motion.

Antigen/antibody reactions occur at the active center in the protein portion. Therefore, the reaction at this active center should be more activated at the stage of contact with the antigen. In a relatively large number of cases, specimens such as viruses are collected in a captured state in a solvent. The specimen is introduced onto a graphene substrate linked with a protein prepared as a sensor.

Therefore, the rotational motion at the linker portion should be more active in a solution consisting of a solvent having higher polarity, and this will lead to an increase in the probability that the active center of the antigen/antibody reaction reacts with the antigen. To realize a good temperature condition, the barrier height should be close to or even less than 0.3 eV. Reducing the barrier height may be achieved by optimizing the solution to achieve nearly equal stability in between two conformations. Selection of a solute with a solvent, e.g., those considered in reference [9] can be a solution. Therefore, it is desirable to select the solvent and temperature conditions so that the probability of appearance of conformation II increases as well as conformation 2 in the protein capture step.

On the other hand, at the time of sensing, the proteins and sample antigens bound by the linker should be strongly bound on the graphene surface. This makes it easier to observe the increased mass by generating a reflected wave with a strong amplitude relative to the incident elastic wave. Therefore, it is advisable to adjust the protein portion containing the supplemented antibody to be on the graphene surface corresponding to conformation I by evaporating the solvent or by changing the temperature and gas pressure conditions. To convert all reacted sites in the planer conformation I at the detection stage, we may dry the sensor system by controlling the external gas pressure.

Here, we mention another merit that a pyrene derivative has for another type of biosensor. In immobilizing proteins on graphene, a pyrene derivative has another merit: non-covalent functionalization, i.e., weaker in bonding with graphene than covalent one for functionalization. Actually, widely employed covalent functionalization may not be suitable for a special purpose [26]. This approach is known to have an undesirable effect of disturbing the electronic properties of graphene [15]. On the other hand, in non-covalent functionalization, the electronic properties of graphene can be preserved [27-29]. Therefore, the PASE linker and its properties may be relevant for another type of the electronic sensing strategy, such as field effect transistor-based biosensors.

Conclusion

We discussed how an activation barrier appears on the potential energy surface in PASE adsorbed on graphene. The conformational change between two bi-stable PASE structures can be regarded as rotational motion around a C–C bond in the alkyl chain. An origin of an activation barrier is the steric hindrance coming from the proximity of a hydrogen on the pyrene to that on the alkyl group.

We also considered the state after a protein is supplemented, and discussed how a similar potential energy surface to that in PASE is expected. If the supplementation of protein can be regarded as a weak perturbation, the rotational motion is expected to remain and the activation barrier is maintained. Then, the probability of the appearance of conformation 2 relative to conformation 1 and vice versa can be adjusted by arranging the environment such as temperature and solvent.

We provided a guideline for an improvement of a biosensing device. In oscillator-type biosensors, by arranging an appropriate surrounding environment, an improvement of the sensitivity is expected.

Computational Method

The density functional theory (DFT) calculation determined stable atomic configurations of conformation 1 and 2 of PASE on graphene. In the DFT calculation realized by the PWscf code of Quantum ESPRESSO [30-32], the DFT-D3 correlation [33] together with PBEsol functional [34] for the exchange-correlation functional described van der Waals interaction between graphene and pyrene fragment in PASE. Ultrasoft pseudopotentials [35] with the energy cutoff of 35 (350) Ry for the expansion of wavefunction (charge density) described the electron-nuclear interaction. Using the $2 \times 4 \times 1$ k-point mesh of Monkhorst–Pack [36], the Brillouin zone sampling was safely performed. Additional details of calculation conditions may be found in a previous paper [9].

After the structural optimization calculation of the (meta)stable conformations until the Hellman–Feynman force acting on each atom was less than 10^{-6} Ry/Bohr, the nudged elastic band method determined the minimum energy pathway. Intermediate images created by linear interpolation between conformation 1 and 2 were optimized so that each image had lower energy while adequate spaces between neighboring images on the energy surface were kept.

To explore the origin of the activation barrier, we analyzed the structure of the saddle point on the minimum energy pathway. Having conformation 1, 2, and the conformation at the saddle

point, we measured the dihedral angles and the distance between two hydrogen atoms using Xcrysden [10].

Acknowledgements

We are grateful to Prof. H. Ogi, Prof. M. Ohtani, Prof. N. Nakamura, Prof. K. Tanigaki, Prof. S. Hagiwara, and Prof. K. Nakajima for fruitful discussions. The calculations were done at the computer centers of Kyushu University and ISSP, University of Tokyo.

Funding

This work is partly supported by JSPS KAKENHI Grant No. JP22K04864.

Author Contributions

Yasuhiro Oishi: formal analysis; investigation; visualization; writing – original draft. Motoharu Kitatani: investigation; software; validation; writing – review & editing. Koichi Kusakabe: conceptualization; methodology; project administration; supervision; writing – original draft.

ORCID® iDs

Koichi Kusakabe - https://orcid.org/0000-0002-0206-8864

Data Availability Statement

The data that supports the findings of this study is available from the corresponding author upon reasonable request.

Preprint

A non-peer-reviewed version of this article has been previously published as a preprint: https://doi.org/10.3762/bxiv.2023.59.v1

References

1. Chen, R. J.; Zhang, Y.; Wang, D.; Dai, H. *J. Am. Chem. Soc.* **2001,** *123,* 3838–3839. doi:10.1021/ja010172b
2. Parviz, D.; Das, S.; Ahmed, H. S. T.; Irin, F.; Bhattacharia, S.; Green, M. J. *ACS Nano* **2012,** *6,* 8857–8867. doi:10.1021/nn302784m
3. Jaegfeldt, H.; Kuwana, T.; Johansson, G. *J. Am. Chem. Soc.* **1983,** *105,* 1805–1814. doi:10.1021/ja00345a021
4. Katz, E. *J. Electroanal. Chem.* **1994,** *365,* 157–164. doi:10.1016/0022-0728(93)02975-n
5. Kodali, V. K.; Scrimgeour, J.; Kim, S.; Hankinson, J. H.; Carroll, K. M.; de Heer, W. A.; Berger, C.; Curtis, J. E. *Langmuir* **2011,** *27,* 863–865. doi:10.1021/la1033178
6. Fan, W.; Zhang, R. *Sci. China, Ser. B: Chem.* **2008,** *51,* 1203–1210. doi:10.1007/s11426-008-0140-2
7. Karachevtsev, V. A.; Stepanian, S. G.; Glamazda, A. Y.; Karachevtsev, M. V.; Eremenko, V. V.; Lytvyn, O. S.; Adamowicz, L. *J. Phys. Chem. C* **2011,** *115,* 21072–21082. doi:10.1021/jp207916d
8. Wu, G.; Tang, X.; Meyyappan, M.; Lai, K. W. C. Chemical functionalization of graphene with aromatic molecule. In *Proceedings of the 2015 IEEE 15th International Conference on Nanotechnology IEEE-NANO,* Rome, July 27–30, 2015; IEEE, 2016; pp 1324–1327. doi:10.1109/nano.2015.7388878
9. Oishi, Y.; Ogi, H.; Hagiwara, S.; Otani, M.; Kusakabe, K. *ACS Omega* **2022,** *7,* 31120–31125. doi:10.1021/acsomega.2c03257
10. Kokalj, A. *J. Mol. Graphics Modell.* **1999,** *17,* 176–179. doi:10.1016/s1093-3263(99)00028-5
11. Murashima, K.; Murakami, M.; Ogi, H.; Kusakabe, K. Carbon-based material vibrator. A sensor element having the same and a biological-substance detection device having the same. U.S. Patent Application US 2021/0223212 A1, July 22, 2021.
12. Haraguchi, T.; Nagakubo, A.; Murashima, K.; Murakami, M.; Ogi, H. 3Pa2-2 Development of 30-GHz phonon biosensor using graphite thin-film resonator. In *Proceedings of Symposium on Ultrasonic Electronics, Vol. 42,* J-Stage: Japan, 2021. doi:10.24492/use.42.0_3pa2-2
13. Mohanty, N.; Berry, V. *Nano Lett.* **2008,** *8,* 4469–4476. doi:10.1021/nl802412n
14. Castro Neto, A. H.; Guinea, F.; Peres, N. M. R.; Novoselov, K. S.; Geim, A. K. *Rev. Mod. Phys.* **2009,** *81,* 109–162. doi:10.1103/revmodphys.81.109
15. Georgakilas, V.; Otyepka, M.; Bourlinos, A. B.; Chandra, V.; Kim, N.; Kemp, K. C.; Hobza, P.; Zboril, R.; Kim, K. S. *Chem. Rev.* **2012,** *112,* 6156–6214. doi:10.1021/cr3000412
16. Wang, Y.; Li, Z.; Wang, J.; Li, J.; Lin, Y. *Trends Biotechnol.* **2011,** *29,* 205–212. doi:10.1016/j.tibtech.2011.01.008
17. Myung, S.; Solanki, A.; Kim, C.; Park, J.; Kim, K. S.; Lee, K.-B. *Adv. Mater. (Weinheim, Ger.)* **2011,** *23,* 2221–2225. doi:10.1002/adma.201100014
18. Yang, W.; Ratinac, K. R.; Ringer, S. P.; Thordarson, P.; Gooding, J. J.; Braet, F. *Angew. Chem., Int. Ed.* **2010,** *49,* 2114–2138. doi:10.1002/anie.200903463
19. Peña-Bahamonde, J.; Nguyen, H. N.; Fanourakis, S. K.; Rodrigues, D. F. *J. Nanobiotechnol.* **2018,** *16,* No. 75. doi:10.1186/s12951-018-0400-z
20. Szunerits, S.; Boukherroub, R. *Interface Focus* **2018,** *8,* 20160132. doi:10.1098/rsfs.2016.0132
21. Kuila, T.; Bose, S.; Khanra, P.; Mishra, A. K.; Kim, N. H.; Lee, J. H. *Biosens. Bioelectron.* **2011,** *26,* 4637–4648. doi:10.1016/j.bios.2011.05.039
22. Chen, S.; Zhang, Z.-B.; Ma, L.; Ahlberg, P.; Gao, X.; Qiu, Z.; Wu, D.; Ren, W.; Cheng, H.-M.; Zhang, S.-L. *Appl. Phys. Lett.* **2012,** *101,* 154106. doi:10.1063/1.4759147
23. Ohno, Y.; Maehashi, K.; Yamashiro, Y.; Matsumoto, K. *Nano Lett.* **2009,** *9,* 3318–3322. doi:10.1021/nl901596m
24. Geim, A. K.; Novoselov, K. S. *Nat. Mater.* **2007,** *6,* 183–191. doi:10.1038/nmat1849
25. Novoselov, K. S.; Geim, A. K.; Morozov, S. V.; Jiang, D.; Zhang, Y.; Dubonos, S. V.; Grigorieva, I. V.; Firsov, A. A. *Science* **2004,** *306,* 666–669. doi:10.1126/science.1102896
26. Loh, K. P.; Bao, Q.; Ang, P. K.; Yang, J. *J. Mater. Chem.* **2010,** *20,* 2277–2289. doi:10.1039/b920539j
27. Liu, J.; Bibari, O.; Mailley, P.; Dijon, J.; Rouvière, E.; Sauter-Starace, F.; Caillat, P.; Vinet, F.; Marchand, G. *New J. Chem.* **2009,** *33,* 1017–1024. doi:10.1039/b813085j
28. Tournus, F.; Latil, S.; Heggie, M. I.; Charlier, J.-C. *Phys. Rev. B* **2005,** *72,* 075431. doi:10.1103/physrevb.72.075431
29. Zhou, L.; Mao, H.; Wu, C.; Tang, L.; Wu, Z.; Sun, H.; Zhang, H.; Zhou, H.; Jia, C.; Jin, Q.; Chen, X.; Zhao, J. *Biosens. Bioelectron.* **2017,** *87,* 701–707. doi:10.1016/j.bios.2016.09.025

30. Giannozzi, P.; Baroni, S.; Bonini, N.; Calandra, M.; Car, R.; Cavazzoni, C.; Ceresoli, D.; Chiarotti, G. L.; Cococcioni, M.; Dabo, I.; Dal Corso, A.; de Gironcoli, S.; Fabris, S.; Fratesi, G.; Gebauer, R.; Gerstmann, U.; Gougoussis, C.; Kokalj, A.; Lazzeri, M.; Martin-Samos, L.; Marzari, N.; Mauri, F.; Mazzarello, R.; Paolini, S.; Pasquarello, A.; Paulatto, L.; Sbraccia, C.; Scandolo, S.; Sclauzero, G.; Seitsonen, A. P.; Smogunov, A.; Umari, P.; Wentzcovitch, R. M. *J. Phys.: Condens. Matter* **2009,** *21,* 395502. doi:10.1088/0953-8984/21/39/395502
31. Giannozzi, P.; Andreussi, O.; Brumme, T.; Bunau, O.; Buongiorno Nardelli, M.; Calandra, M.; Car, R.; Cavazzoni, C.; Ceresoli, D.; Cococcioni, M.; Colonna, N.; Carnimeo, I.; Dal Corso, A.; de Gironcoli, S.; Delugas, P.; DiStasio, R. A., Jr.; Ferretti, A.; Floris, A.; Fratesi, G.; Fugallo, G.; Gebauer, R.; Gerstmann, U.; Giustino, F.; Gorni, T.; Jia, J.; Kawamura, M.; Ko, H.-Y.; Kokalj, A.; Küçükbenli, E.; Lazzeri, M.; Marsili, M.; Marzari, N.; Mauri, F.; Nguyen, N. L.; Nguyen, H.-V.; Otero-de-la-Roza, A.; Paulatto, L.; Poncé, S.; Rocca, D.; Sabatini, R.; Santra, B.; Schlipf, M.; Seitsonen, A. P.; Smogunov, A.; Timrov, I.; Thonhauser, T.; Umari, P.; Vast, N.; Wu, X.; Baroni, S. *J. Phys.: Condens. Matter* **2017,** *29,* 465901. doi:10.1088/1361-648x/aa8f79
32. Giannozzi, P.; Baseggio, O.; Bonfà, P.; Brunato, D.; Car, R.; Carnimeo, I.; Cavazzoni, C.; de Gironcoli, S.; Delugas, P.; Ferrari Ruffino, F.; Ferretti, A.; Marzari, N.; Timrov, I.; Urru, A.; Baroni, S. *J. Chem. Phys.* **2020,** *152,* 154105. doi:10.1063/5.0005082
33. Grimme, S.; Antony, J.; Ehrlich, S.; Krieg, H. *J. Chem. Phys.* **2010,** *132,* 154104. doi:10.1063/1.3382344
34. Perdew, J. P.; Ruzsinszky, A.; Csonka, G. I.; Vydrov, O. A.; Scuseria, G. E.; Constantin, L. A.; Zhou, X.; Burke, K. *Phys. Rev. Lett.* **2008,** *100,* 136406. doi:10.1103/physrevlett.100.136406
35. Vanderbilt, D. *Phys. Rev. B* **1990,** *41,* 7892–7895. doi:10.1103/physrevb.41.7892
36. Monkhorst, H. J.; Pack, J. D. *Phys. Rev. B* **1976,** *13,* 5188–5192. doi:10.1103/physrevb.13.5188

License and Terms